AGU100 ADVANCING EARTH AND SPACE SCIENCE

Geophysical Research Letters

RESEARCH LETTER
10.1029/2018GL079938

Key Points:
- We make the first estimate of global radiation balance and surface temperature response to vegetation damage by ozone
- Radiative changes are dominated by atmospheric moisture and cloud response to ozone-induced changes in plant transpiration
- Ozone-vegetation-hydrology interactions should be considered in future climate scenarios and simulations

Supporting Information:
- Supporting Information S1

Correspondence to:
S. R. Arnold,
s.arnold@leeds.ac.uk

Citation:
Arnold, S. R., Lombardozzi, D., Lamarque, J.-F., Richardson, T., Emmons, L. K., Tilmes, S., et al. (2018). Simulated global climate response to tropospheric ozone-induced changes in plant transpiration. *Geophysical Research Letters*, *45*. https://doi.org/10.1029/2018GL079938

Received 6 AUG 2018
Accepted 25 NOV 2018
Accepted article online 28 NOV 2018

Simulated Global Climate Response to Tropospheric Ozone-Induced Changes in Plant Transpiration

S. R. Arnold[1], D. Lombardozzi[2], J.-F. Lamarque[3,4], T. Richardson[1], L. K. Emmons[3], S. Tilmes[3], S. A. Sitch[5], G. Folberth[6], M. J. Hollaway[7], and M. Val Martin[8]

[1]Institute for Climate and Atmospheric Science, School of Earth and Environment, University of Leeds, Leeds, UK, [2]Terrestrial Sciences Section, National Center for Atmospheric Research, Boulder, CO, USA, [3]Atmospheric Chemistry and Observations Modeling Laboratory, National Center for Atmospheric Research, Boulder, CO, USA, [4]Climate and Global Dynamics Division, National Center for Atmospheric Research, Boulder, CO, USA, [5]College of Life and Environmental Sciences, University of Exeter, Exeter, UK, [6]Hadley Centre, Met Office, Exeter, UK, [7]Lancaster Environment Centre, Lancaster University, Lancaster, UK, [8]Chemical and Biological Engineering Department, University of Sheffield, Sheffield, UK

Abstract Tropospheric ozone (O_3) pollution is known to damage vegetation, reducing photosynthesis and stomatal conductance, resulting in modified plant transpiration to the atmosphere. We use an Earth system model to show that global transpiration response to near-present-day surface tropospheric ozone results in large-scale global perturbations to net outgoing long-wave and incoming shortwave radiation. Our results suggest that the radiative effect is dominated by a reduction in shortwave cloud forcing in polluted regions, in response to ozone-induced reduction in land-atmosphere moisture flux and atmospheric humidity. We simulate a statistically significant response of annual surface air temperature of up to ~ +1.5 K due to this ozone effect in vegetated regions subjected to ozone pollution. This mechanism is expected to further increase the net warming resulting from historic and future increases in tropospheric ozone.

Plain Language Summary Ozone is a pollutant near the Earth's surface, where it is harmful to health and vegetation. Ozone is formed by chemical reactions in the atmosphere driven by the action of sunlight on emissions from fossil fuel combustion and other sources. Ozone harms vegetation by entering leaves through small pores on leaves called stomata. These stomata are also the route by which gases such as water vapor and CO_2 are naturally exchanged between plants and the atmosphere. Ozone damage to vegetation affects the efficiency with which gases pass through plant stomata, typically reducing both photosynthesis and stomatal conductance due to biochemical damage. This results in a change in the amount of water vapor that plants put into the atmosphere. In this study we use a computer model to estimate for the first time how this modification in plant water vapor source to the atmosphere changes climate. We show widespread surface warming and changes in clouds due to the impact of ozone on plants. This has important implications for policies aimed at limiting global and regional temperature increases in the presence of ozone pollution and provides evidence for an additional climate benefit to reducing ozone pollution.

1. Introduction

Tropospheric ozone (O_3) is a secondary air pollutant, formed by photochemical oxidation of CO, methane, and other volatile organic compounds in the presence of nitrogen oxides ($NO + NO_2$; Lelieveld & Dentener, 2000). Increased emissions of ozone precursors since the Industrial Revolution have led to large-scale enhancements in ozone throughout the troposphere (Young et al., 2013), resulting in net warming of climate, with an estimated global mean radiative forcing of 0.4 W/m^2 (0.2 to 0.6 W/m^2, 95% CI; Myhre et al., 2013). Ozone at the surface is harmful to human health (Anenberg et al., 2010; Tjoelker et al., 1995) and also damages vegetation, reducing plant photosynthesis and crop yields (Bowen, 1926; Hollaway et al., 2012). This reduction in photosynthesis inhibits the land carbon sink, leading to an indirect climate forcing resulting from an enhancement in atmospheric CO_2 (Sitch et al., 2007).

Stomatal cells regulate carbon entering and water exiting plant leaves, and respond to changes light, temperature, and carbon dioxide concentrations (Jones, 1998). Exposure to enhanced near-surface atmospheric ozone concentrations has been shown to reduce leaf-level stomatal conductance, inhibiting trace gas exchange between the plant leaf surface and atmosphere (Hoshika et al., 2015; Lombardozzi et al., 2013;

Wittig et al., 2007). Previous studies have demonstrated impacts of enhanced near-surface atmospheric ozone on watershed runoff and soil water content, resulting from ozone-induced changes in vegetation transpiration (Bernacchi et al., 2011; Felzer et al., 2009).

The extent to which large-scale exposure of vegetation to enhanced ozone may have implications for the global water cycle and climate system via impacts on global land-atmosphere moisture fluxes has so far not been be quantified. Model studies suggest a widespread perturbation to global plant transpiration through ozone-induced changes in stomatal conductance (Hoshika et al., 2015; Huntingford et al., 2011; Lombardozzi et al., 2012; Lombardozzi et al., 2015). In addition to inducing stomatal closure, observations show that ozone can inhibit stomatal control, leading to less efficient stomatal response to other environmental controls (so-called sluggish stomata; Hoshika et al., 2015; Paoletti & Grulke, 2005). Stomatal sluggishness may lead to reduced stomatal closure under stress, such as drought conditions, resulting in further ozone uptake and water loss. Loss of stomatal control occurs due to direct ozone damage to leaf-level biochemical pathways, leading to a decoupling of stomatal conductance response from photosynthesis response (Paoletti, 2005; Tjoelker et al., 1995). It is important to account for this decoupling, since it leads to a modified large-scale transpiration response to ozone compared with approaches where stomatal responses are coupled to ozone-induced photosynthetic decreases (Lombardozzi et al., 2012). So far, no study has investigated the implications of ozone-induced changes in surface moisture fluxes for global atmospheric moisture and climate under a realistic tropospheric ozone distribution and accounting for decoupling of stomatal and photosynthesis ozone responses. Here we use a coupled atmosphere-land surface model to estimate the global climate response to ozone-induced changes in plant-atmosphere moisture fluxes for a year 2000 near-present-day scenario, using a parameterization that includes empirically derived functions to account separately for stomatal and photosynthetic responses to plant ozone uptake.

2. Model Simulations and Ozone Evaluation

2.1. Model Setup

We use the Community Earth System Model (CESM; http://www2.cesm.ucar.edu/) version 1.1.1 to make the first estimate of the global climate response to ozone-induced changes in plant-atmosphere moisture fluxes. The model includes full coupling between the atmospheric model component (Community Atmosphere Model (CAM) 4; Neale et al., 2013) and the land surface and vegetation model (Community Land Model [CLM] 4.0; Oleson et al., 2010). Surface fluxes of heat, moisture, and momentum to the atmosphere and surface albedo are calculated by CLM4 and passed directly to CAM4. Similarly, radiation, humidity, precipitation, surface air temperature (SAT), and trace gas concentrations (including model-simulated tropospheric O_3) are passed from CAM4 to the vegetation simulation in CLM4. This allows plant photosynthesis and stomatal conductance to respond to simulated atmospheric ozone from CAM4, and the CAM4 atmospheric moisture budget to respond to simulated changes in land surface fluxes from CLM4. CAM4 simulates tropospheric ozone photochemistry, using an online tropospheric chemistry scheme (CAM-Chem; Lamarque et al., 2012), based on the MOZART-4 chemical mechanism (Emmons et al., 2010). The model used here includes dry deposition driven by model-simulated stomatal conductance from CLM4, updated and optimized with leaf area index (LAI; Val Martin et al., 2014). Prescribed monthly sea surface temperatures (SSTs) and sea ice distributions for year 2000 are specified, generated by Community Climate System Model version 4 for the Coupled Model Intercomparison Project Phase 5 (Meehl et al., 2012). The fixed SST approach allows us to isolate the so-called *fast response* of climate to ozone-induced changes in vegetation transpiration from relatively short time-slice integrations. Note that this does not account for longer term equilibrium climate response via SST changes. Our diagnosed top-of-atmosphere (TOA) radiative changes are therefore equivalent to effective radiative forcing, as defined by the Intergovernmental Panel on Climate Change (Myhre et al., 2013). Trace gas and aerosol emissions for year 2000 are taken from Lamarque et al. (2011). Simulated changes in ozone and aerosol do not feed back onto model radiation and the climate simulation, or affect LAI, vegetation biomass, or vegetation distribution. Simulated changes in aerosol do not affect cloud properties. The version of CLM4 used here employs a fixed vegetation plant functional type distribution for the year 2000 based on the HYDE (History Database of the Global Environment) version 3.0 database (Lawrence et al., 2012) and satellite phenology to prescribe, rather than active biogeochemistry to predict, leaf area indices (Oleson et al., 2010). Evapotranspiration in CLM4 is partitioned between ground evaporation, canopy evaporation, and transpiration (see Figure S2 in the supporting information), with model updates to improve partitioning between

10.1029/2018GL079938

transpiration and evaporation components (Lawrence et al., 2007). Our simulations have no active nitrogen cycle or biomass allocation; however, photosynthesis and stomatal conductance are simulated online.

2.2. Ozone Damage Parameterization

A parameterization for ozone effects on photosynthesis and stomatal conductance is included following previous off-line studies using CLM, which have evaluated ozone effects on global vegetation productivity and surface fluxes (Lombardozzi et al., 2012; Lombardozzi et al., 2015). Ozone-induced vegetation damage is related to plant ozone flux—here a cumulative uptake of ozone (CUO). Flux has been shown to more reliably relate to reduction in plant photosynthesis compared with atmospheric ozone concentration-based exposure (Karlsson et al., 2007). CUO to plant leaves is accumulated when ozone flux exceeds a 0.8 $\mathrm{nmol \cdot m^{-2} \cdot s^{-1}}$ threshold value (Lombardozzi et al., 2015), over the growing season (defined as when total LAI is greater than 0.5; Lombardozzi et al., 2012). CUO is related to leaf stomatal resistance for water vapor (r_s), by

$$\mathrm{CUO} = \boldsymbol{\Sigma}\,(k_{\mathrm{O3}}/r_{\mathrm{s}}).[\mathrm{O_3}] \tag{1}$$

where k_{O3} is the ratio of ozone and water leaf resistances and $[O_3]$ is the simulated surface level atmospheric ozone concentration from CAM4.

Photosynthesis and stomatal conductance CUO response curves are derived from a previously compiled empirical data set for three different vegetation types: deciduous, evergreen, and grass (Lombardozzi et al., 2013). The Ball-Woodrow-Berry model approach (Ball et al., 1987) used in CLM4 calculates stomatal conductance based on photosynthetic rates. Since stomatal conductance often does not decrease in response to ozone at the same rate as photosynthesis, we use a previously developed methodology to modify the stomatal conductance response to CUO independently of photosynthesis (Lombardozzi et al., 2012; Lombardozzi et al., 2015). This explicit separation has been neglected by some previous studies, but is of importance here, since it leads to a modified stomatal and transpiration response to ozone compared with approaches where transpiration responses are coupled to photosynthetic decreases (Lombardozzi et al., 2012).

While the model configuration used here allows diagnosis of global impacts of ozone on plant stomatal conductance and transpiration, it should be recognized that there are uncertainties in the formulation of the CLM ozone response function. Plant responses are based on empirical data for three broad plant functional type responses (for deciduous, evergreen, and grass/crops; Lombardozzi et al., 2015), and primarily on chamber experiment-derived dose-response relationships under high ozone, where responses may be different from those found in the natural environment. Nevertheless, we present the first results documenting the important feedback of ozone-plant interactions on the large-scale hydrological cycle using a state-of-the-art scheme.

2.3. Model Experiments and Ozone Evaluation

Our focus is on physical climate response to ozone vegetation effects. A similar model setup was recently used to evaluate atmospheric chemistry responses to ozone effects on vegetation (Sadiq et al., 2017). We compare a model simulation that includes ozone effects on photosynthesis and stomatal conductance with a simulation in which this parameterization is not applied, to quantify the effects of the ozone-induced modification to surface moisture fluxes on simulated climate. We conduct two simulations, each 22 years in length, using repeating year 2000 emissions, SSTs, and ice cover. Our base simulation does not account for vegetation damage by ozone, and a second simulation includes the ozone-induced effects on photosynthesis and stomatal conductance, based on the simulated CUO. For each simulation, we present annual averages of 21 years of monthly output. Following a 1-year spin-up, we find no statistically significant trends in model output over the 21-year period analyzed. We calculate statistical significance of monthly differences between the two simulations using a Student's t test on 21 years of output from each simulation, setting a significance threshold of $p < 0.05$. In addition, we discount significance for gridpoints that display any significant degree of temporal autocorrelation ($p < 0.05$) over the 21-year simulation.

The simulated distribution of surface ozone (Figure 1a) shows enhancements over and downstream of polluted regions of the Northern Hemisphere (NH). We compare simulated surface ozone concentrations with a collection of surface ozone observations from Europe, North America, Japan, and Southern Hemisphere midlatitude sites (Figure S1). Within each region, 1995–2005 ozone observations from stations at altitudes

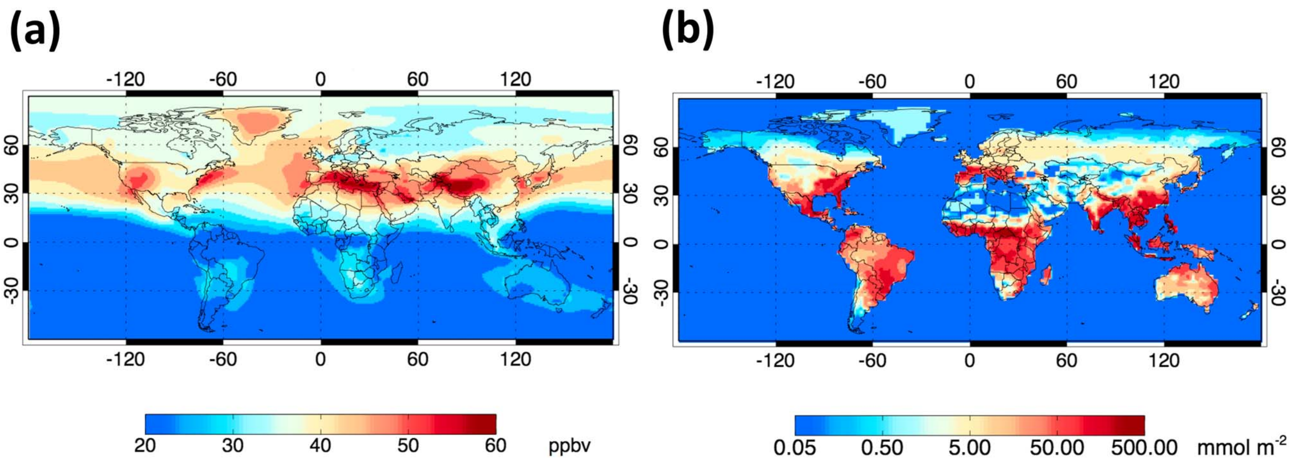

Figure 1. Simulated annual mean surface (a) ozone concentrations and (b) cumulative stomatal ozone flux.

less than 500 m above sea level are compared with 21-year average model-simulated surface ozone, interpolated to observation locations. Further details on observations are given in Figure S1 and in Tilmes et al. (2012). Model surface ozone concentrations compare well with observations from Europe, Asia, and the Southern Hemisphere, with a more substantial overestimate over North America. However, overall mean bias is small (3.6 ppbv, 11%), with modeled and observed ozone concentration distributions overlapping within their interannual variabilities in all locations and months.

3. Climate Response to Plant Ozone Damage

3.1. Impacts on Land Surface Fluxes

Simulated enhancements in surface ozone over continental regions imply the potential for widespread impacts of ozone on plant photosynthesis and transpiration. Since ozone flux is determined by both atmospheric ozone concentration and leaf stomatal conductance, relatively low ozone concentrations may produce substantial fluxes and plant damage in regions where stomatal uptake is particularly efficient (Paoletti & Grulke, 2005). The results of this effect are evident in differences between simulated spatial patterns of surface ozone concentrations and cumulative leaf ozone uptake (Figures 1a and 1b). Most notably, despite tropical surface ozone concentrations being substantially smaller than those at mid latitudes, the tropics display large leaf ozone uptake, due to larger stomatal conductances, leaf lifespan, and a longer growing season.

Globally, the inclusion of the ozone-vegetation effect produces a reduction in latent heat (LH) flux (-0.31 ± 0.2 W/m^2, global mean and interannual variability (IAV), and all gridpoints), which is offset by an equal increase in sensible heat flux ($+0.31 \pm 0.12$ W/m^2, global mean and IAV, and all gridpoints). This is equivalent to a large scale repartitioning between LH and sensible heat (a change in the so-called *Bowen ratio*; Bowen, 1926). This repartitioning is particularly evident in regions of enhanced surface ozone (Figures 2a and 2b). A large-scale repartitioning in evaporative land-atmosphere moisture flux occurs when including the ozone effect. Large decreases in fractional contribution from canopy transpiration are partly offset by an increase in fractional contribution from ground evaporation (Figure S2), due to an increase in land surface moisture resulting from the decrease in transpiration land-atmosphere moisture flux. Statistically robust decreases in plant transpiration in response to ozone occur in widespread locations across the NH and tropics, with the strongest decreases in eastern United States, extratropical South America, and tropical Africa (Figure 2c). A previous model study using CLM 4.5 similarly showed strong transpiration response in eastern United States (Lombardozzi et al., 2015). Our simulations provide the first global estimate of transpiration response to ozone where feedback between changes in model climate and surface vegetation processes are included. In particular, transpiration in our simulations is affected by simulated changes in atmospheric humidity and vapor pressure deficit, which have a direct control on stomatal conductance (Jarvis, 1976; Li & Li, 2014).

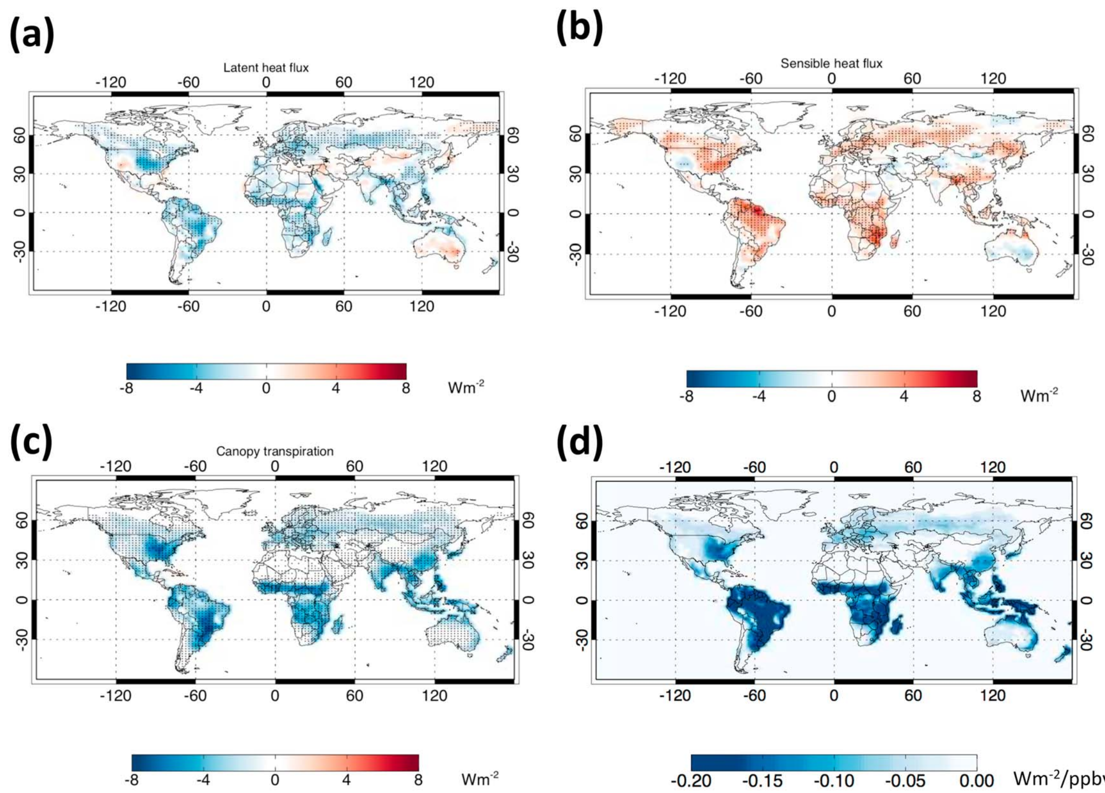

Figure 2. Annual mean ozone-induced differences (ozone on-ozone off) in (a) surface latent heat flux, (b) surface sensible heat flux, (c) transpiration, and (d) transpiration difference normalized by simulated surface atmospheric ozone mixing ratio. Stippling in panels (a-c) denotes regions where 21-year mean differences are significant ($p \leq 0.05$).

The simulated reduction in transpiration in response to a given concentration of surface ozone is strongly regionally dependent. Figure 2d shows simulated changes in annual mean canopy transpiration normalized by surface ozone concentration. Tropical ecosystems show a larger absolute reduction in transpiration per ppbv surface ozone, as a result of larger stomatal conductance and leaf uptake over the year. In addition, a high proportion of evergreen vegetation in the tropics means that longer leaf lifetimes allow cumulative ozone uptake over longer periods (typically 2–3 years), compared with shorter accumulation ($<$1 year) in deciduous vegetation, which is more prevalent at midlatitudes. While cumulative ozone uptake tends to be larger in tropical regions, there is much more variability in the transpiration response compared with midlatitudes, particularly at high CUO (see Figure S3). Available empirical tropical tree response data show similarly large uncertainty and CUO range (Lombardozzi et al., 2013).

3.2. Impacts on Atmosphere Radiative Fluxes and Temperature Response

Inclusion of plant ozone uptake and its effects in the model results in a small global annual mean TOA net radiative effect of +0.04 ± 0.32 (IAV) W/m^2 with substantial IAV. The global mean net radiative effect results from an increase in net downward shortwave (SW) radiation of 0.19 ± 0.32 (IAV) W/m^2, partly offset by an increase in outgoing long-wave (LW) radiation of 0.15 ± 0.11 (IAV) W/m^2. The spatial pattern of changes in model TOA LW and SW radiative fluxes resulting from ozone effects on vegetation and regional temperature response is shown in Figure 3. Regionally, there are more robust changes, with extensive areas of statistical significance near to regions of enhanced ozone. Statistically significant increases in annual mean 2-m SAT resulting from the ozone vegetation are simulated in the same broad regions (North America, Western Europe, East Asia, Amazon, Central Africa, and Eastern Siberia; Figure 3c). The land surface temperature response shows a similar spatial pattern, to that of SAT, with slightly larger magnitudes simulated over the continents (Figure S4), The large increases in SAT simulated over N America are consistent with regional model experiments for summertime continental United States in which regional-scale changes in heat and

10.1029/2018GL079938

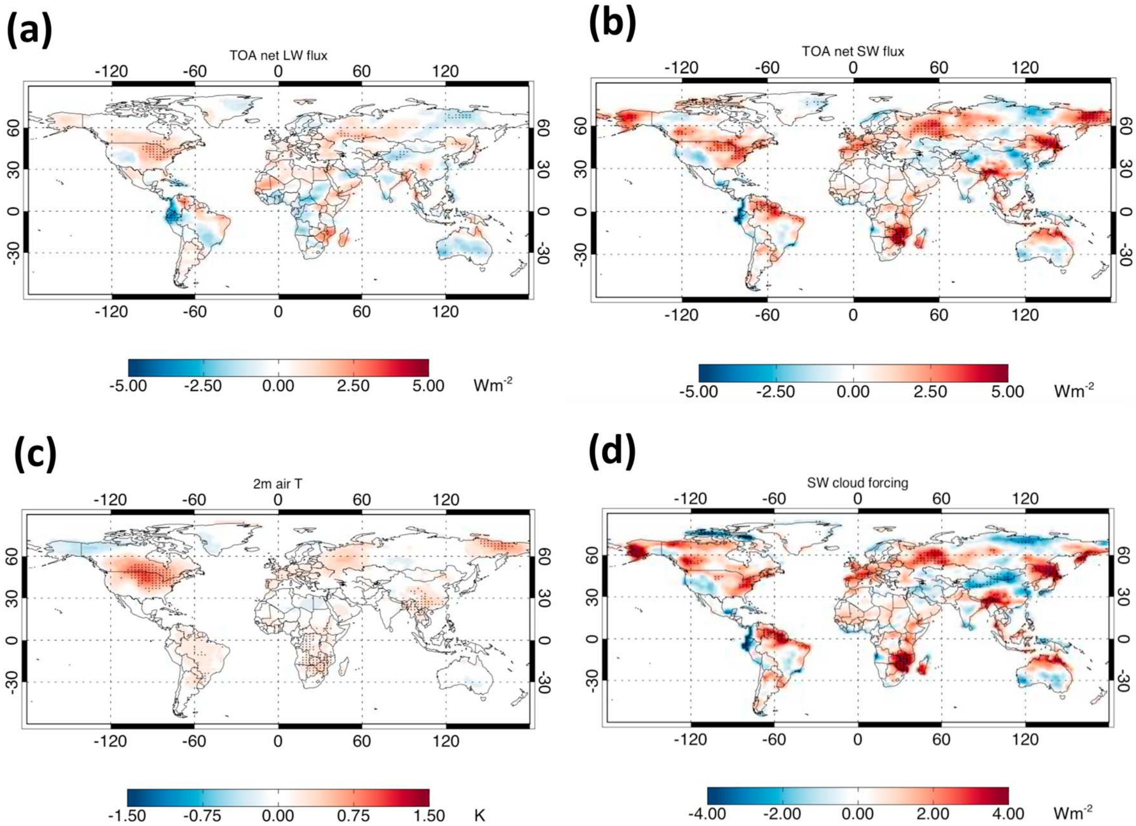

Figure 3. Annual mean ozone-induced differences (ozone on-ozone off) in (a) top-of-atmosphere net outgoing long-wave (LW) flux, (b), top-of-atmosphere net downward shortwave (SW) flux, (c) 2-m surface air temperature, and (d) SW cloud forcing. Stippling denotes regions where 21-year mean differences are significant ($p \leq 0.05$).

moisture flux as a result of chronic vegetation ozone exposure were investigated (Li et al., 2016). Below, we explore the mechanism driving the widespread global SAT responses in our simulations.

The global radiative changes produced by the ozone vegetation damage effect are dominated by regional atmospheric responses to the surface flux repartitioning. Such responses include LW response to ozone-induced changes in atmospheric water vapor and the atmospheric temperature profile, and LW and SW responses to changes in clouds. In addition, effects of SW response to changes in albedo resulting from snow cover differences (sea ice and glaciers are fixed in our simulations) caused by changes in atmospheric moisture and temperature play a role in some regions (see Figure S5).

As expected in temperate and tropical regions, the spatial pattern and magnitude of the SW radiative change (Figure 3b) closely match changes in SW cloud forcing (Figure 3d; $r^2 = 0.98$ between 60°S and 60°N). However, changes in clear-sky SW radiative flux (Figure S5) show that a large portion of the SW response over snow-covered high-latitude North America and Siberia is instead due to surface albedo changes. The dominance of cloud effects in the SW response implies that warming in regions of enhanced ozone pollution at midlatitudes and in the tropics is essentially driven by reductions in cloud cover resulting from ozone-induced changes in moisture flux to the atmosphere. This mechanism is consistent with previous idealized experiments in CAM 3.1, in which large-scale cooling was simulated in response to an increase in low-level cloud under artificially imposed increases in surface LH fluxes (Ban-Weiss et al., 2011). Largest statistically robust SW radiative effects and temperature responses are simulated in North America, Europe, Eastern Siberia, East Asia, Amazonia, and Central Africa. These are regions with extensive areas of vegetation, where ozone precursor emissions are also present, either from anthropogenic or biomass burning sources (Granier et al., 2011). Comparing changes in clear-sky LW flux (Figure S5) and all-sky LW flux (Figure 3a) shows that regional patterns of increasing and decreasing LW flux in the tropics are also dominated by cloud changes. These changes lead to both positive and negative LW response in tropical regions, compared with a more

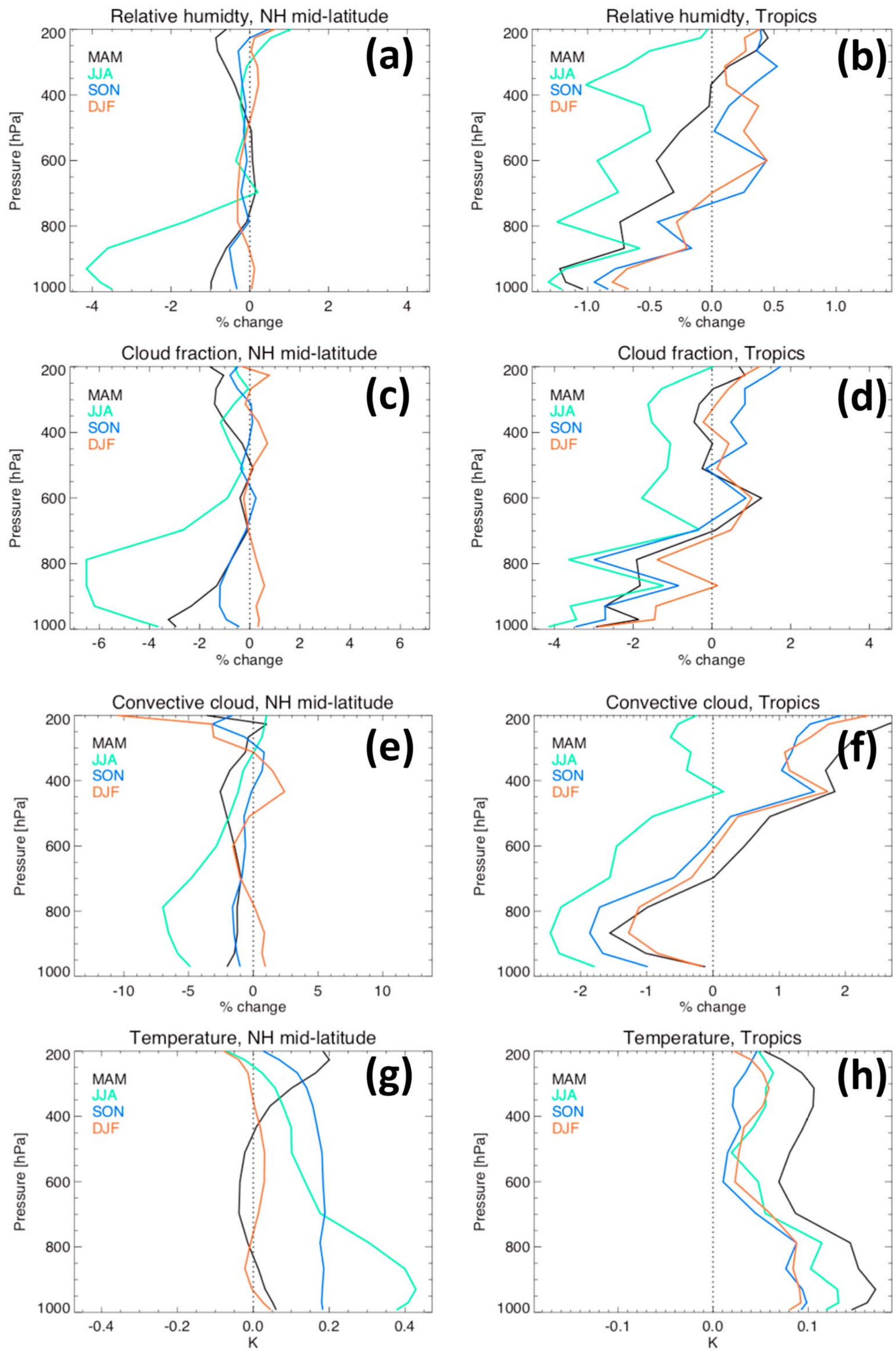

Figure 4. Average ozone-induced changes in profiles of (a and b) relative humidity, (c and d) total cloud fraction, (e and f) convective cloud fraction, (g and h) temperature, for (a, c, e, and g) northern midlatitude (30°–60°N) and (b, d, f, and h) tropical (30°S–30°N) land gridpoints. Fractional (%) changes in quantities are shown except for temperature where absolute (K) changes are shown.

10.1029/2018GL079938

dominant negative LW response in the extratropics, likely as a result of upper level convective cloud response in the tropics (see below). The result is less offset of the positive SW response in tropical regions compared with the extratropics.

Vertical profiles of changes in humidity, cloudiness, and temperature further support linkages between cloud cover and temperature response, driven by changes in atmospheric moisture. Figure 4 shows changes in NH midlatitude (30°–60°N) and tropical (30°S–30°N) tropospheric profiles over land grid points, of relative humidity, total cloud fraction, convective cloud fraction, and temperature, produced by the ozone impact on plant transpiration. At midlatitudes, drying of the lower troposphere from the ozone impact on transpiration is strongest in summer, when transpiration is most efficient and surface ozone is also enhanced. This drying is coincident with large reductions in low cloud fraction and increased temperatures, suggestive of warming produced via increased SW heating at the surface under reduced cloud. Winter (December-January-February) sees minimum profile changes at midlatitudes, when plant photosynthesis and transpiration (as well as ozone) are lowest, and large regions of frozen ground limit land-atmosphere moisture flux. The large simulated SAT change in North America (Figure 3c) results from a combination of the decrease in cloud fraction during summer and a widespread decrease in albedo due to reduced snow cover in winter (see Figure S5). The SAT response is Eastern Siberia is mostly driven by changes in snow cover and albedo (Figure S5), with only a small contribution from SW cloud forcing (Figure 3d). In the tropics, the atmospheric moisture and cloud changes are more complex, due to the increased role of convective cloud in the radiation budget, and convective response to changes in the temperature profile. The result is that a shift in the tropical temperature profile leads to enhanced convective cloud in the middle/upper troposphere (700–200 hPa), which partly offsets the reduction in low-level cloud fraction. Seasonality in the tropical response is substantially smaller than at midlatitudes.

4. Discussion and Conclusions

The simulated increased sensitivity of transpiration to ozone in the tropics has potential implications for climate response to future changes in tropospheric ozone. Future projections of ozone precursor emissions imply ozone reductions in midlatitudes, and increases in industrializing tropical regions (Lamarque et al., 2011), highlighting the need for focused data collection on ozone-vegetation interactions in tropical regions. Increased ozone production efficiency from precursor emissions at lower latitudes (Paoletti, 2005) may also compound vegetation effects due to an equatorward redistribution of emissions. Even at midlatitudes, efforts to reduce surface ozone through implementation of clean air legislation may be offset by the effects of a warming climate (Val Martin et al., 2015) or by global methane increases (Fiore et al., 2002), which may result in increased ozone concentrations and consequent impacts on extra-tropical transpiration. Further Earth system model simulations are required to investigate how future ozone impacts on transpiration may act alongside the effects of increases in CO_2 via its role in reducing stomatal conductance (Jones, 1998) and more complex responses to temperature change and changes in availability of water and nutrients.

These model results advance our understanding of the complex interdependencies between atmospheric chemistry, the biosphere, and physical climate. We have made the first assessment of worldwide regional climate impacts from tropospheric ozone effects on plant transpiration, which we propose as an additional mechanistic link between degradation in surface air quality and atmospheric moisture and surface temperature change. Our findings provide further support for cobenefits to climate and public health that could result from legislation aimed at reducing ozone precursor emissions (Huntingford et al., 2011) and may imply that more stringent controls on ozone precursor emissions are required to meet future temperature targets, particularly regionally. Further work is required to fully evaluate this mechanism and the resulting climatic response empirically, including attempts to quantify impacts of ozone-vegetation interactions on regional moisture and radiation budgets using observations. Our model simulations provide regional information on where the proposed mechanism may be important, and a challenge will be to empirically isolate this effect from other drivers of variability in the moisture and radiative budgets. Furthermore, there is an urgent need to better constrain the stomatal response of vegetation to ozone empirically, particularly for tropical plant species, for which our simulations predict the largest transpiration response per ppbv ozone, but for which there is limited empirical constraint on the parameterized sensitivity to ozone. Future Earth system model studies will be required to investigate climate feedbacks resulting from ozone-induced changes in atmospheric moisture and clouds on longer timescales, and how these effects act alongside the expected impacts of ozone on the carbon cycle (Collins et al., 2010; Sitch et al., 2007). Our results demonstrate that ozone-vegetation-hydrology interactions need to be considered in future projections of climate change, particularly in regions of enhanced ozone pollution, and in assessments of climate mitigation potential of ozone precursor emission controls.

Data availability

Twenty-one-year average model output and evaluation data used in this study are available on request via ftp from University of Leeds.

Acknowledgments
This work was supported by the UK Natural Environment Research Council (NE/H020241/1). S. R. Ay acknowledges support from the National Center for Atmospheric Research (NCAR) visitor program and an NCAR Advanced Study Program Faculty Fellowship award. Support was also provided by U.S. Department of Energy grants DE-FC03-97ER62402/A010 and DE-SC0012972 and the National Institute of Food and Agriculture/U.S. Department of Agriculture grants 2015-67003-23489 and 2015-67003-23485. The National Center for Atmospheric Research is funded by the National Science Foundation.

References

Anenberg, S. C., Horowitz, L. W., Tong, D. Q., & West, J. J. (2010). An estimate of the global burden of anthropogenic ozone and fine particulate matter on premature human mortality using atmospheric modeling. *Environmental Health Perspectives*, *118*(9), 1189–1195. https://doi.org/10.1289/ehp.0901220

Ball, J. T., Woodrow, I. E., & Berry, J. A. (1987). A model predicting stomatal conductance and its contribution to the control of photosynthesis under different environmental conditions. In J. Biggins (Ed.), *Progress in photosynthesis research: Volume 4 Proceedings of the VIIth International Congress on Photosynthesis Providence, Rhode Island, USA, August 10–15, 1986*, (pp. 221–224). Dordrecht: Springer Netherlands. https://doi.org/10.1007/978-94-017-0519-6_48

Ban-Weiss, G. A., Govindasamy, B., Long, C., Pongratz, J., & Caldeira, K. (2011). Climate forcing and response to idealized changes in surface latent and sensible heat. *Environmental Research Letters*, *6*(3), 034032. https://doi.org/10.1088/1748-9326/6/3/034032

Bernacchi, C. J., Leakey, A. D. B., Kimball, B. A., & Ort, D. R. (2011). Growth of soybean at future tropospheric ozone concentrations decreases canopy evapotranspiration and soil water depletion. *Environmental Pollution*, *159*(6), 1464–1472. https://doi.org/10.1016/j.envpol.2011.03.011

Bowen, I. S. (1926). The ratio of heat losses by conduction and by evaporation from any water surface. *Physical Review*, *27*(6), 779–787. https://doi.org/10.1103/PhysRev.27.779

Collins, W. J., Sitch, S., & Boucher, O. (2010). How vegetation impacts affect climate metrics for ozone precursors. *Journal of Geophysical Research*, *115*, D23308. https://doi.org/10.1029/2010JD014187

Emmons, L. K., Walters, S., Hess, P. G., Lamarque, J. F., Pfister, G. G., Fillmore, D., Granier, C., et al. (2010). Description and evaluation of the model for ozone and related chemical tracers, version 4 (MOZART-4). *Geoscientific Model Development*, *3*(1), 43–67. https://doi.org/10.5194/gmd-3-43-2010

Felzer, B. S., Cronin, T. W., Melillo, J. M., Kicklighter, D. W., & Schlosser, C. A. (2009). Importance of carbon-nitrogen interactions and ozone on ecosystem hydrology during the 21st century. *Journal of Geophysical Research*, *114*, G01020. https://doi.org/10.1029/2008JG000826

Fiore, A. M., Jacob, D. J., Field, B. D., Streets, D. G., Fernandes, S. D., & Jang, C. (2002). Linking ozone pollution and climate change: The case for controlling methane. *Geophysical Research Letters*, *29*(19), 1919. https://doi.org/10.1029/2002GL015601

Granier, C., Bessagnet, B., Bond, T., D'Angiola, A., Denier van der Gon, H., Frost, G. J., Heil, A., et al. (2011). Evolution of anthropogenic and biomass burning emissions of air pollutants at global and regional scales during the 1980–2010 period. *Climatic Change*, *109*(1-2), 163–190. https://doi.org/10.1007/s10584-011-0154-1

Hollaway, M. J., Arnold, S. R., Challinor, A. J., & Emberson, L. D. (2012). Intercontinental trans-boundary contributions to ozone-induced crop yield losses in the Northern Hemisphere. *Biogeosciences*, *9*(1), 271–292. https://doi.org/10.5194/bg-9-271-2012

Hoshika, Y., Katata, G., Deushi, M., Watanabe, M., Koike, T., & Paoletti, E. (2015). Ozone-induced stomatal sluggishness changes carbon and water balance of temperate deciduous forests. *Scientific Reports*, *5*(1), 9871. https://doi.org/10.1038/srep09871

Huntingford, C., Cox, P. M., Mercado, L. M., Sitch, S., Bellouin, N., Boucher, O., & Gedney, N. (2011). Highly contrasting effects of different climate forcing agents on terrestrial ecosystem services. *Philosophical Transactions of the Royal Society A: Mathematical, Physical and Engineering Sciences*, *369*(1943), 2026–2037. https://doi.org/10.1098/rsta.2010.0314

Jarvis, P. G. (1976). The interpretation of the variations in leaf water potential and stomatal conductance found in canopies in the Field. *Philosophical Transactions of the Royal Society, B: Biological Sciences*, *273*(927), 593–610. https://doi.org/10.1098/rstb.1976.0035

Jones, H. G. (1998). Stomatal control of photosynthesis and transpiration. *Journal of Experimental Botany*, *49*, 387–398.

Karlsson, P. E., Braun, S., Broadmeadow, M., Elvira, S., Emberson, L., Gimeno, B. S., le Thiec, D., et al. (2007). Risk assessments for forest trees: The performance of the ozone flux versus the AOT concepts. *Environmental Pollution*, *146*(3), 608–616. https://doi.org/10.1016/j.envpol.2006.06.012

Lamarque, J. F., Emmons, L. K., Hess, P. G., Kinnison, D. E., Tilmes, S., Vitt, F., Heald, C. L., et al. (2012). CAM-chem: Description and evaluation of interactive atmospheric chemistry in the Community Earth System Model. *Geoscientific Model Development*, *5*(2), 369–411. https://doi.org/10.5194/gmd-5-369-2012

Lamarque, J.-F., Kyle, G. P., Meinshausen, M., Riahi, K., Smith, S. J., van Vuuren, D. P., Conley, A. J., et al. (2011). Global and regional evolution of short-lived radiatively-active gases and aerosols in the Representative Concentration Pathways. *Climatic Change*, *109*(1-2), 191–212. https://doi.org/10.1007/s10584-011-0155-0

Lawrence, D. M., Thornton, P. E., Oleson, K. W., & Bonan, G. B. (2007). The partitioning of evapotranspiration into transpiration, soil evaporation, and canopy evaporation in a GCM: Impacts on land–atmosphere interaction. *Journal of Hydrometeorology*, *8*(4), 862–880. https://doi.org/10.1175/JHM596.1

Lawrence, P. J., Feddema, J. J., Bonan, G. B., Meehl, G. A., O'Neill, B. C., Oleson, K. W., Levis, S., et al. (2012). Simulating the biogeochemical and biogeophysical impacts of transient land cover change and wood harvest in the community climate system model (CCSM4) from 1850 to 2100. *Journal of Climate*, *25*(9), 3071–3095. https://doi.org/10.1175/JCLI-D-11-00256.1

Lelieveld, J., & Dentener, F. J. (2000). What controls tropospheric ozone? *Journal of Geophysical Research*, *105*(D3), 3531–3551. https://doi.org/10.1029/1999JD901011

Li, J., & Li, X. (2014). Response of stomatal conductance of two tree species to vapor pressure deficit in three climate zones. *Journal of Arid Land*, *6*(6), 771–781. https://doi.org/10.1007/s40333-014-0030-8

Li, J., Mahalov, A., & Hyde, P. (2016). Simulating the impacts of chronic ozone exposure on plant conductance and photosynthesis, and on the regional hydroclimate using WRF/Chem. *Environmental Research Letters*, *11*(11), 114017. https://doi.org/10.1088/1748-9326/11/11/114017

Lombardozzi, D., Levis, S., Bonan, G., Hess, P. G., & Sparks, J. P. (2015). The influence of chronic ozone exposure on global carbon and water cycles. *Journal of Climate*, *28*(1), 292–305. https://doi.org/10.1175/JCLI-D-14-00223.1

Lombardozzi, D., Levis, S., Bonan, G., & Sparks, J. P. (2012). Predicting photosynthesis and transpiration responses to ozone: Decoupling modeled photosynthesis and stomatal conductance. *Biogeosciences*, *9*(8), 3113–3130. https://doi.org/10.5194/bg-9-3113-2012

Lombardozzi, D., Sparks, J. P., & Bonan, G. (2013). Integrating O3 influences on terrestrial processes: Photosynthetic and stomatal response data available for regional and global modeling. *Biogeosciences*, *10*(11), 6815–6831. https://doi.org/10.5194/bg-10-6815-2013

Meehl, G. A., Hu, A., Tebaldi, C., Arblaster, J. M., Washington, W. M., Teng, H., Sanderson, B. M., et al. (2012). Relative outcomes of climate change mitigation related to global temperature versus sea-level rise. *Nature Climate Change*, *2*(8), 576–580. https://doi.org/10.1038/nclimate1529

Myhre, G., Shindell, D., Bréon, F.-M., Collins, W., Fuglestvedt, J., Huang, J., et al. (2013). Anthropogenic and natural radiative forcing. In T. F. Stocker, D. Qin, G.-K. Plattner, M. Tignor, S. K. Allen, J. Boschung, A. Nauels, Y. Xia, V. Bex, & P. M. Midgley (Eds.), *Climate change 2013: The physical science basis. Contribution of Working Group I to the Fifth Assessment Report of the Intergovernmental Panel on Climate Change*, (pp. 659–740). Cambridge, UK, and New York: Cambridge Univ. Press.

Neale, R. B., Richter, J., Park, S., Lauritzen, P. H., Vavrus, S. J., Rasch, P. J., & Zhang, M. (2013). The mean climate of the Community Atmosphere Model (CAM4) in forced SST and fully coupled experiments. *Journal of Climate*, *26*(14), 5150–5168. https://doi.org/10.1175/JCLI-D-12-00236.1

Oleson, K. W., Lawrence, D. M., Bonan, G. B., Flanner, M. G., Kluzek, E., Lawrence, P. J., et al. (2010), Technical description of version 4.0 of the Community Land Model (CLM), NCAR Technical Note.

Paoletti, E. (2005). Ozone slows stomatal response to light and leaf wounding in a Mediterranean evergreen broadleaf, Arbutus unedo. *Environmental Pollution*, *134*(3), 439–445. https://doi.org/10.1016/j.envpol.2004.09.011

Paoletti, E., & Grulke, N. E. (2005). Does living in elevated CO_2 ameliorate tree response to ozone? A review on stomatal responses. *Environmental Pollution*, *137*(3), 483–493. https://doi.org/10.1016/j.envpol.2005.01.035

Sadiq, M., Tai, A. P. K., Lombardozzi, D., & Val Martin, M. (2017). Effects of ozone-vegetation coupling on surface ozone air quality via biogeochemical and meteorological feedbacks. *Atmospheric Chemistry and Physics*, *17*, 3055–3066. https://doi.org/10.5194/acp-17-3055-2017

Sitch, S., Cox, P. M., Collins, W. J., & Huntingford, C. (2007). Indirect radiative forcing of climate change through ozone effects on the land-carbon sink. *Nature*, *448*(7155), 791–794. https://doi.org/10.1038/nature06059

Tilmes, S., Lamarque, J.-F., Emmons, L. K., Conley, A., Schultz, M. G., Saunois, M., Thouret, V., et al. (2012). Technical note: Ozonesonde climatology between 1995 and 2011: Description, evaluation and applications. *Atmospheric Chemistry and Physics*, *12*(16), 7475–7497, https://doi.org/10.5194/acp-12-7475-2012

Tjoelker, M. G., Volin, J. C., Oleksyn, J., & Reich, P. B. (1995). Interaction of ozone pollution and light effects on photosynthesis in a forest canopy experiment. *Plant, Cell & Environment*, *18*(8), 895–905. https://doi.org/10.1111/j.1365-3040.1995.tb00598.x

Val Martin, M., Heald, C. L., & Arnold, S. R. (2014). Coupling dry deposition to vegetation phenology in the Community Earth System Model: Implications for the simulation of surface O3. *Geophysical Research Letters*, *41*, 2988–2996. https://doi.org/10.1002/2014GL059651

Val Martin, M., Heald, C. L., Lamarque, J. F., Tilmes, S., Emmons, L. K., & Schichtel, B. A. (2015). How emissions, climate, and land use change will impact mid-century air quality over the United States: A focus on effects at national parks. *Atmospheric Chemistry and Physics*, *15*(5), 2805–2823. https://doi.org/10.5194/acp-15-2805-2015

Wittig, V. E., Ainsworth, E. A., & Long, S. P. (2007). To what extent do current and projected increases in surface ozone affect photosynthesis and stomatal conductance of trees? A meta-analytic review of the last 3 decades of experiments. *Plant, Cell & Environment*, *30*(9), 1150–1162. https://doi.org/10.1111/j.1365-3040.2007.01717.x

Young, P. J., Archibald, A. T., Bowman, K. W., Lamarque, J. F., Naik, V., Stevenson, D. S., Tilmes, S., et al. (2013). Pre-industrial to end 21st century projections of tropospheric ozone from the Atmospheric Chemistry and Climate Model Intercomparison Project (ACCMIP). *Atmospheric Chemistry and Physics*, *13*(4), 2063–2090. https://doi.org/10.5194/acp-13-2063-2013